SAXS Analysis of the Thermal Relaxation of Anisotropic Morphologies in Oriented Nafion Membranes

Kirt A. Page,[†] Forrest A. Landis,[‡] Alan K. Phillips,[†] and Robert B. Moore*,[†]

Department of Polymer Science, The University of Southern Mississippi, Hattiesburg, Mississippi 39406-0076, and Polymers Division, National Institute of Standards and Technology, 100 Bureau Dr., Gaithersburg, Maryland 20899

Received November 4, 2005; Revised Manuscript Received March 17, 2006

ABSTRACT: The current study uses variable temperature, small-angle X-ray scattering (SAXS) to examine the thermal relaxation behavior of oriented Nafion films as a means to evaluate the morphological stability of this ionomer at elevated temperatures. The SAXS patterns of uniaxially oriented films are characterized by strong equatorial scattering peaks which are attributed to scattering arising from the oriented ionic domains (ionomer peak ca. $q = 2$ nm^{-1}). The intensity of the equatorial peaks—obtained from integration in the azimuthal direction (χ)—and the degree of orientation—calculated using the Hermans orientation function (f)—were monitored as a function of temperature. At lower temperatures, a constant value of f and a correlation between the β relaxation and a slight decrease in the scattering intensity of the equatorial peaks are in agreement with our earlier assignment of the β relaxation to the T_g of Nafion. At temperatures in the vicinity of the β relaxation, the static electrostatic network inhibits long-range molecular relaxation and yields a persistent anisotropic morphology. In contrast, significant changes in intensity of the equatorial peaks and values of the orientation parameter at elevated temperatures were shown to correlate well with the α relaxation observed in DMA. At temperatures in the vicinity of the α relaxation, a significant destabilization of the oriented electrostatic network occurs (i.e., through the activation of a dynamic network involving significant ion-hopping processes), thus facilitating the observed relaxation to an isotropic morphology. Therefore, morphological stability in this ionomer is principally governed by the thermal stability of the electrostatic network and not the glass transition.

Introduction

The most widely studied perfluorosulfonate ionomer (PFSI)[1−3] is 1100 equiv weight Nafion, which is a product of the Dupont Chemical Company, having the following structure (where equivalent weight, EW, is the grams of dry polymer per equivalent of SO_3^- groups).

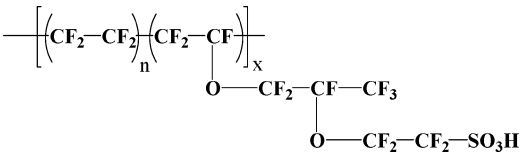

Because of Coulombic interactions, the polar perfluoroether side chains containing the ionic, sulfonate groups have been shown to aggregate, leading to a nanophase-separated morphology where the ionic domains, termed clusters,[4] are distributed throughout the nonpolar poly(tetrafluoroethylene) (PTFE) matrix. In addition, the runs of tetrafluoroethylene, of sufficient length, are capable of organizing into crystalline domains having unit cell dimensions virtually identical to that of pure PFTE.[5,6] This complex, phase-separated morphology of PFSI's, consisting of crystalline and ionic domains, has been the focus of several investigations aimed at characterizing the morphology[4,6−18] and the thermomechanical[19−25] behavior of these technologically important materials.

Numerous morphological studies of Nafion have focused on the small-angle X-ray scattering behavior of this unique ionomer.[4,6−18] With electron density differences between the ionic domains and the PTFE matrix, a scattering maximum appears in small-angle X-ray scattering profiles at ca. $q = 1-2$ nm^{-1}, which has been termed the "ionomer peak". In addition, a very low angle peak or shoulder is often observed at ca. $q = 0.5$ nm^{-1}, which has been attributed to scattering from the locally ordered crystallites composed of relatively long runs of PTFE segments between side chains.[4,7] Several structural models have been proposed in order to explain the origins of the ionomer peak in Nafion;[4,6−18] however, for the purposes of this study, it is only necessary that the ionomer peak be attributed to the existence of ionic aggregates that are distributed throughout the matrix with some degree of spatial heterogeneity. With respect to thermal and mechanical properties, these ionic domains are generally accepted to constitute the electrostatic network within PFSI's (i.e., physical cross-links that can inhibit segmental mobility).

Because of the complex nature of the morphology of Nafion, several studies have attempted to elucidate and/or verify structural models by manipulating the morphology through processes such as solvent swelling and mechanical deformation. For the purpose of this paper, discussion will be aimed at those investigations involving mechanical deformation of Nafion films (specifically, uniaxial extension). In particular, several groups have shown the effect of uniaxial deformation on the small- and wide-angle X-ray scattering behavior of the Nafion membranes in an attempt to evaluate the size, shape, and spatial distribution of crystallites and ionic domains in Nafion.[4,8,13,26−31]

Gierke et al.[4] were the first to report the effect of uniaxial deformation on the SAXS data of the unhydrolyzed Nafion precursor and hydrolyzed ionomer. For the oriented nonionic

[†] The University of Southern Mississippi.
[‡] National Institute of Standards and Technology.
* To whom all correspondence should be addressed: e-mail rbmoore@usm.edu; Ph 601-266-4480; Fax 601-266-5635.

10.1021/ma052359j CCC: $33.50
Published on Web 04/27/2006

precursor, the low q peak attributed to intercrystalline domain scattering (often referred to as the long period) at ca. 0.5 nm^{-1} was observed only in the meridional scan, implying periodicity in the long period in the direction of orientation. However, in the case of the hydrolyzed ionomer, scans revealed that the ionomer peak was only observed in the equatorial plane, which implies periodicity of the ionic domains perpendicular to the orientation direction.

Fujimura and co-workers[8] conducted SAXS studies on cesium-neutralized Nafion in which the draw ratio λ_b (i.e., the ratio of the final, extended length to the initial, undrawn length) was systematically varied up to a value of $\lambda_b = 1.5$. As the draw ratio was increased, the ionomer peak was observed to shift to lower angles and decrease in intensity in the meridional (orientation) direction while in the equatorial direction the intensity of the ionomer peak increased and shifted to higher angles. By using Bragg's law to calculate interdomains spacings from the peak maxima, a nonaffine deformation behavior was observed between the microscopic dimensions and the macroscopic deformation (i.e., draw length). This observation led to the conclusion that nonaffine behavior was inconsistent with a model attributing scattering to interparticle interference but supported a model in which scattering arose from intraparticle interference (i.e., a core−shell particle).

Elliot and co-workers[13,29] performed detailed SAXS investigations of the morphology of Nafion membranes subjected to uniaxial and biaxial orientation. In agreement with earlier studies, the ionomer peak was shown to exhibit a significant degree of anisotropy upon deformation and the anisotropy was observed to increase with increasing orientation. This behavior was explained on the basis of an interparticle scattering model and was contrasted to the behavior predicted for models involving intraparticle scattering. The interparticle scattering model described the anisotropic scattering in terms of an increase in the coherence of the interparticle spacing orthogonal to the orientation direction, accompanied by a corresponding reduction in the coherence in the parallel direction.[13] In a further communication, Elliot et al.[29] found that unaxially oriented membranes could relax back to an almost isotropic state when swollen with ethanol/water mixtures. However, membranes swollen in water alone showed no morphological relaxation. This behavior was attributed to the ability of ethanol to plasticize the fluorocarbon matrix of Nafion.

Londono et al.[32] reported synchrotron SAXS studies of oriented Nafion in which an increase in elongation (up to 150%) was shown to lead to a disappearance of the ionomer peak in the meridional direction and coupled with a narrowing of the ionomer peak azimuthally. At the highest elongation, an equatorial steak—similar to that seen in SAXS of drawn fibers containing microfibrils—was observed. Scattering profiles were obtained along orthogonal orientations of the films. Isotropic scattering in the direction of orientation led to confirmation of the fibrillar morphology of the Nafion films. From further analysis, the authors suggested that the morphology of uniaxially oriented Nafion consists of oriented cylindrical or lamellar domains, rather than spherical clusters.

Computational methods combined with a novel approach in the application of scattering physics were recently employed by Barbi et al.[26] in a synchrotron SAXS study of Nafion as a function of mechanical load. The deformation behavior was evaluated over a range of elongations (0−125%), and a description of the deformation mechanism was proposed in the context of the classical ionomer domain model of Gierke (i.e., ionic clusters represented by spheres and connected by nanochannels). The channels were proposed to open and widen in the direction of orientation while simultaneously merging with adjacent domains to form slab-shaped domains, which align in the direction of orientation.

Moore and co-workers[27,28,31,33] have reported that Nafion membranes neutralized with alkylammonium ions could be highly oriented at elevated temperatures (achieving λ_b values in excess of 5) to yield anisotropic scattering patterns as measured by WAXD and SAXS. Upon cooling to room temperature, the extremely oriented morphology was found to persist in free-standing films. As the degree of orientation was increased, the scattering intensity of the ionomer peak—as measured by a 2-dimensional area detector—was shown to increase profoundly in the equatorial direction, while scattering in the meridional direction was shown to effectively disappear. A circular integration over all azimuthal angles of the scattering patterns was preformed to calculate the scattering invariant for samples having a range of elongations. An increase in the scattering invariant with increasing elongation was attributed to a higher degree of ionic aggregation that yielded a matrix with fewer lone pairs, relative to the undrawn state.[27]

Recently, Diat and co-workers[30] have used simultaneous synchrotron small/wide-angle scattering to look the structural orientation of uniaxially stretched Nafion films. The analysis in the small-angle region focused on the ionomer peak, while analysis in the wide-angle region focused on the amorphous and crystalline peaks as well as a peak labeled peak 3, which was attributed to several diffraction peaks resulting from intramolecular correlations. Several interesting observations were made regarding the ionomer, amorphous, crystalline, and peak 3 positions during the drawing process. The crystalline peak position in the meridional and equatorial directions was observed to remain constant during the drawing process. However, the ionomer, amorphous, and peak 3 positions were shown to decrease in the meridional direction with increasing draw ratio. An analysis of the scattering intensity in the azimuthal direction (between 0 and 90°) shows an increase in the scattering intensity with increasing azimuthal angle for the ionomer, crystalline, and amorphous peaks, whereas peak 3 shows a decrease in scattering intensity. The increase in intensity of the ionomer, amorphous, and crystalline peaks was attributed to more chains being aligned along the meridional direction (i.e., parallel to the drawing direction). Upon further analysis of the Hermans orientation factor, it was shown that the ionomer peak reaches maximum orientation at lower draw ratios than the crystalline peak. On the basis of a fibrillar structure as the model for Nafion morphology[17,18,30] (i.e., elongated polymeric aggregates which can form bundles), a two-step mechanism was proposed to describe the orientation process. At small draw ratios there is a rotation of the bundles followed by an orientation of the aggregates located within the bundles at higher draw ratios.

The above studies have demonstrated how systematic morphological manipulations through uniaxial extension may be used to more fully understand the complex supermolecular organization of Nafion. However, another important aspect of this simple structural manipulation allows for the direct observation of morphological rearrangements that are possible when these materials are subjected to elevated temperatures. As an example of the importance of this fundamental information, these ionomers are the benchmark membrane materials for proton exchange membrane fuel cell (PEMFC) applications. Currently, PEMFC systems are required to maintain operation temperatures of 80−120 °C, and these temperatures are in the

range where the onset of significant molecular mobility is observed.[34] If this molecular mobility can allow for undesirable morphological rearrangements, then extended high-temperature operation could compromise performance and durability. Thus, by understanding the molecular factors that govern morphological stability, strategies to mitigate the possible occurrence of undesirable structural changes in these technologically important membrane materials may be developed.

While uniaxial extension can yield an anisotropic morphology in Nafion that is stable and persistent at room temperature, to date, there have been no complete studies reported on the thermally induced relaxation of anisotropic Nafion films. In this study, time-resolved synchrotron SAXS is used to investigate the thermal relaxation behavior of oriented membranes neutralized with tetramethyl (TMA^+)-, tetraethyl (TEA^+)-, tetrapropyl (TPA^+)-, and tetrabutylammonium (TBA^+) ions as the samples are heated from 50 to 300 °C. The degree of orientation, calculated by the Hermans orientation function (*f*), and the relative intensity of the equatorial scattering peaks were obtained from azimuthal integrations of the anisotropic scattering patterns and are reported as a function of temperature for each of the neutralized samples. These data are compared to dynamic mechanical analysis for the same samples and thus correlated to our previous assignments of the molecular origins of the mechanical relaxations observed for these materials.[34] Through these correlations, we are able to consider morphological stability on the basis of thermally stimulated changes in molecular dynamics within the complex electrostatic network of Nafion.

Experimental Section

Materials. Nafion 117 (1100 EW, sulfonic acid form) was obtained from E.I. DuPont de Nemours & Co. The tetramethyl (TMA^+)-, tetraethyl (TEA^+)-, tetrapropyl (TPA^+)-, and tetrabutylammonium (TBA^+) counterions were obtained from Aldrich in the form of hydroxides dissolved in either water or methanol. All other reagents were obtained from Aldrich and used without further purification.

PFSI Sample Preparation. The PFSI membranes were cleaned by refluxing in 4 M methanolic H_2SO_4 for ca. 12 h. These H^+-form membranes were then boiled in deionized (DI) water for 1 h as washed (3×) to remove excess acid. For neutralization of Nafion membranes with the alkylammonium counterions, the samples were prepared by soaking the H^+-form membranes in excess (ca. 5×) methanolic solution of the appropriate alkylammonium hydroxide. The neutralized membranes were thoroughly rinsed of excess alkylammonium hydroxide with methanol (3×) and dried in a vacuum oven at 70 °C overnight, prior to analysis.

Uniaxial orientation of the alkylammonium neutralized Nafion films were performed on stamped "dog-bone"-shaped samples. Prior to orientation, the central sections of the dog bones were marked with regularly spaced ink lines in order to accurately determine the final draw ratios. The Nafion membranes were oriented to a draw ratio ($\lambda = l/l_0$) of 3, using an in-house designed, uniaxial drawing apparatus with temperature control set at 190, 170, 100, and 80 °C for the TMA^+, TEA^+, TPA^+, and TBA^+ forms, respectively. Immediately after reaching the desired draw ratio, the membranes were rapidly quenched to room temperature.

Dynamic Mechanical Analysis (DMA). Dynamic mechanical measurements were performed using a Seiko Instruments SDM 5600 series dynamic mechanical spectrometer (DMS 200). Membrane samples were analyzed in the tensile mode at a frequency of 1 Hz and a heating rate of 5 °C/min.

Small-Angle X-ray Scattering (SAXS). Variable temperature, time-resolved small-angle X-ray scattering was performed at the Brookhaven National Laboratory on the Advanced Polymer Beamline (X27C) at the National Synchrotron Light Source. The incident X-ray beam was tuned to a wavelength of 0.1366 nm, and the sample-to-detector distance was 85 cm. The two-dimensional scattering images were recorded using a Mar CCD camera with an intensity uncertainty on the order of 2%. The Nafion samples were heated in a sample chamber in the X-ray beam at a heating rate of 5 °C/min with an uncertainty of ±1 °C while acquisition times were kept to 1 min and data were recorded from 50 to 300 °C. Intensity vs pixel, as well as azimuthal angle, data were obtained from the integration of the 2-D images using the POLAR software developed by Stonybrook Technology and Applied Research, Inc. The relationship between pixel and the momentum transfer vector *q* was determined by calibrating the scattering data with a silver behenate standard. All scattering intensities were corrected for transmission, incident beam flux, and background scatter due to air and Kapton windows. The scattering profiles were corrected for transmission and background scatter and are represented in arbitrary, relative intensity units as a function of the scattering vector, *q*, which is a function of the scattering angle through the following relationship:

$$q = \frac{4\pi}{\lambda}\sin(\theta) \tag{1}$$

where λ is the wavelength of radiation (0.1366 nm) and θ is half of the scattering angle (2θ).

The scattering profiles were also integrated azimuthally over a narrow range of scattering vectors in the vicinity of the ionomer peak ($q_{max} \pm 0.4$ nm^{-1}). To analyze the azimuthal plots, a linear baseline was fit to the data and subtracted to facilitate accurate calculation of the orientation function (*f*), which will be discussed later. The data were partitioned into equal parts from 0−180°(χ) and 180−360°(χ). The Hermans orientation function was calculated for each of the equatorial peaks, and the two values were averaged. Because of increases in the level of noise at high temperatures, it was not possible to calculate *f* over the entire temperature range. Therefore, calculations of *f* were carried out only for those scattering profiles where the fluctuation in the baseline intensity (σ) was less than 5% of the maximum peak intensity ($I(\chi)_{max}$).

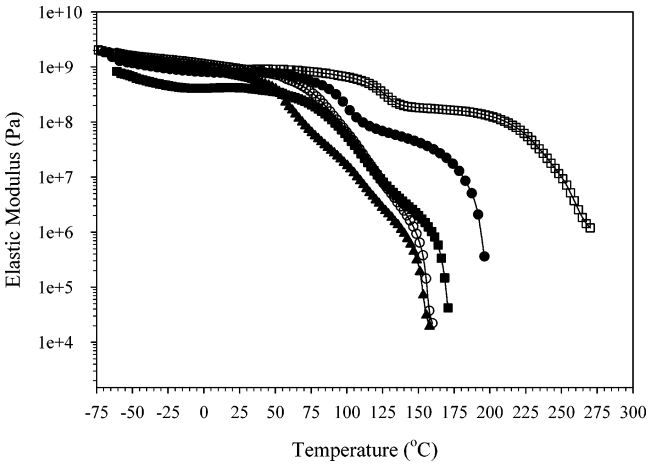

Figure 1. Storage modulus vs temperature for (■) H^+-, (□) TMA^+-, (●) TEA^+-, (○) TPA^+-, and (▲) TBA^+-form Nafion.

Results and Discussion

Dynamic Mechanical Analysis. Figure 1 shows plots of the storage modulus vs temperature for TMA^+, TEA^+, TPA^+, and TBA^+ neutralized Nafion. As a reference, the mechanical data for H^+-form Nafion have also been included. While the mechanical behavior of the neutralized forms are dominated by electrostatic interactions,[34] it is important to recognize that the hydrogen-bonding interactions for the H^+-form of Nafion (i.e., the form used in PEMFC applications) yield behavior well within the range of this specific series of counterion forms. At low temperatures (i.e., less than 50 °C), the storage modulus

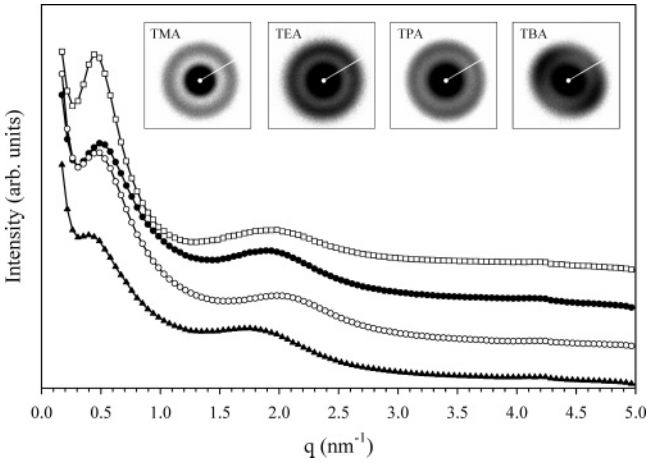

Figure 2. SAXS powder patterns and radial integration profiles (50 °C) for (□) TMA^+-, (●) TEA^+-, (○) TPA^+-, and (▲) TBA^+-form Nafion.

remains high regardless of the counterion type, which is a characteristic behavior of a cross-linked network below its glass transition temperature. The effect of counterion size is most significant in the rubbery modulus and the terminal region. As the size of the counterion increases, the temperature at which the storage modulus drops by several orders of magnitude decreases across the entire temperature range measured. It is also important to note that the transition in the storage modulus (1) decreases in temperature and (2) becomes less distinct with an increase in the counterion size.

Small-Angle X-ray Analysis. Figure 2 shows the relative scattering intensity as a function of scattering vector, q, obtained from radial integrations of the 2-dimensional scattering patterns (displayed as insets) for TMA^+, TEA^+, TPA^+, and TBA^+ Nafion at 50 °C. Each of the scattering profiles contains two distinct scattering maxima occurring at ca. $q = 0.4-0.6$ nm^{-1} and ca. $q = 1.7-2.0$ nm^{-1} and has been attributed to intercrystalline domain scattering (often referred to as the long period) and interparticle scattering from the ionic domains, respectively.[34] In this as-received (unoriented) state, the 2-D scattering patterns are essentially isotropic; however, a slight asymmetry in the ionomer peak is apparent in the TBA^+-form Nafion sample and is indicative of residual orientation in the as-received film due to the manufacturing process (i.e., the machine direction in the extruded films). While interesting differences in the scattering intensity of the peak attributed to the crystalline character are apparent with changes in counterion type, these observations are likely linked to changes in scattering contrast, and a further analysis is outside the scope of this study. Thus, analysis of the oriented films in this study will focus on the scattering peak arising from the ionic domains.

For TMA^+-and TBA^+-form Nafion oriented to a draw ratio of $\lambda_b = 3$, Figure 3 shows the effect of temperature on the anisotropic character of the scattering profiles. In agreement with earlier studies,[4,7,8,13,29,30,32] the anisotropic scattering from the sample heated to 50 °C is characterized by (1) two equatorial spots, which are attributed to scattering arising from the oriented ionic domains (ionomer peak), and (2) low q equatorial streaking, which is attributed to a fibrillar-type morphology.[17,18,30] As the sample is heated, the anisotropic scattering of the ionomer peak, for TMA^+-form Nafion, is shown to persist up to temperatures around 265 °C. However, at temperatures close to 300 °C, the scattering profile transforms into a weak isotropic halo. The scattering for oriented TBA^+-form Nafion (Figure 3) also shows anisotropic scattering at 50

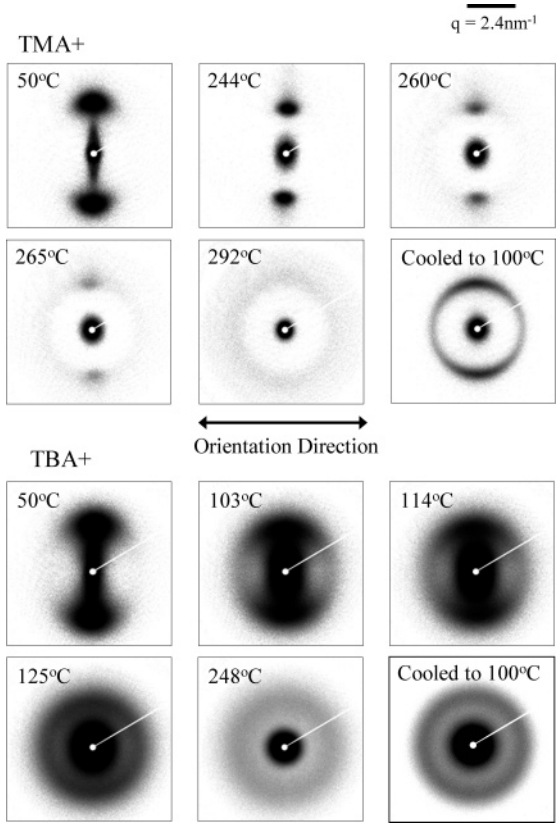

Figure 3. SAXS patterns of oriented ($\lambda_b = 3$) TMA^+- and TBA^+-form Nafion during the heating process and after cooling to 100 °C.

°C, which relaxes during the heating process. However, the relaxation to isotropic scattering occurs at a much lower temperature (ca. 130 deg lower), compared to the TMA^+-form Nafion, and the scattering intensity weakens significantly near 250 °C.

For both the TMA^+- and TBA^+-form Nafion samples in Figure 3, scattering from the ionic domains reappears with increased intensity upon cooling, and the 2-D patterns are clearly observed to be more isotropic, relative to the initial oriented state. This behavior suggests that the spatial distribution of ion pairs is significantly disrupted at elevated temperatures, yielding a more homogeneous distribution (i.e., with characteristic weak scattering), yet the reassociation into distinct aggregates is reversible upon cooling. Moreover, this thermally stimulated redistribution of ion pairs allows for a profound morphological rearrangement back to a more isotropic morphology similar to that observed for the unoriented samples. From a qualitative inspection of the uncorrected, 2-dimensional scattering patterns it can be seen that as the size of the counterion increases (1) the equatorial arc due to orientation becomes broader in the azimuthal direction (χ), indicating a decreasing degree of orientation, and (2) the temperature at which relaxation to an isotropic morphology occurs decreases. The lower degree of residual orientation observed as the counterion size increases can be explained by the ability of the larger counterions to facilitate greater chain mobility.[34] Because of the greater chain mobility, there is a significant degree of stress relaxation that can occur during the orienting and thermal annealing processes, thus leading to a less oriented morphology in the final state (after cooling to room temperature).

Figure 4A−D shows the variable temperature azimuthal plots for TMA^+, TEA^+, TPA^+, and TBA^+ Nafion, respectively. Each of the samples shows strong equatorial scattering peaks located

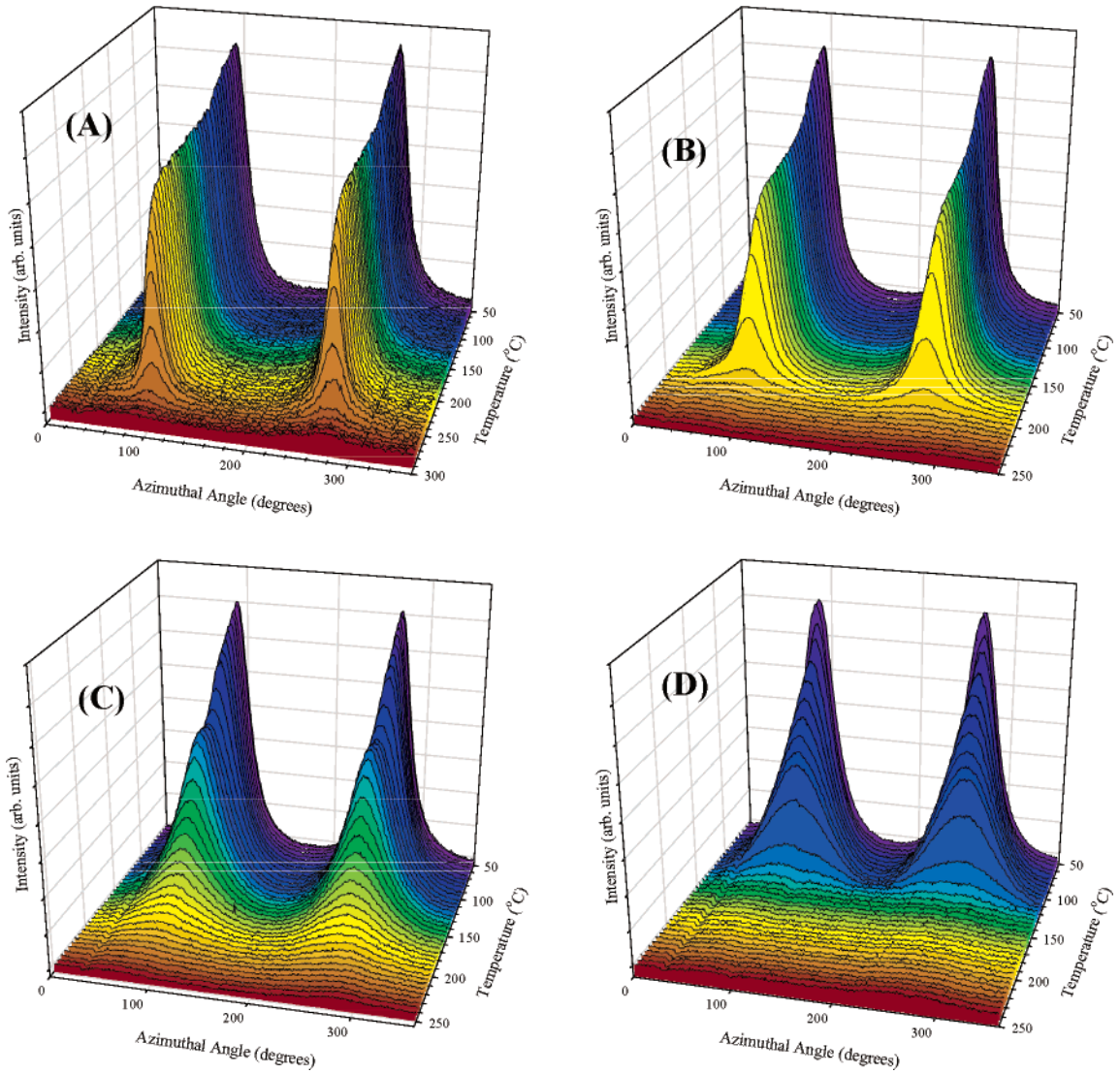

Figure 4. Variable temperature SAXS for scattering in the azimuthal direction (χ) for (A) TMA^+-, (B) TEA^+-, (C) TPA^+-, and (D) TBA^+-form Nafion.

at approximately 90°and 270° (χ) with respect to the orientation direction. These peaks arise from correlations in the direction perpendicular to orientation and are attributed to orientation of the ionic domains parallel to the orientation direction. For each counterion form, the anisotropic scattering from the highly oriented samples transforms, at elevated temperatures, into isotropic profiles with a uniform distribution of scattered intensity over all azimuthal angles. Moreover, the temperatures at which these sudden transformations occur are found to decrease with increasing counterion size.

A more direct comparison of the temperature-dependent scattering behavior can be seen in Figure 5 as plots of the maximum intensity of the equatorial peak in the range of 180−360°(χ) as a function of temperature. These data are characterized by a "two-tiered" decrease in the scattering intensity with increasing temperature (similar to that seen for the storage modulus in Figure 1), and the temperature range over which the changes in intensity occurs decreases with increasing counterion size. For example, the equatorial peak for TMA^+ Nafion shows a drop in intensity up to ca. 125 °C, where it reaches a plateau persisting up to ca. 240 °C, above which the intensity drops off in a rapid, stepwise fashion. This behavior is also observed for the other alkylammonium neutralized samples, although the plateau narrows as the counterion size

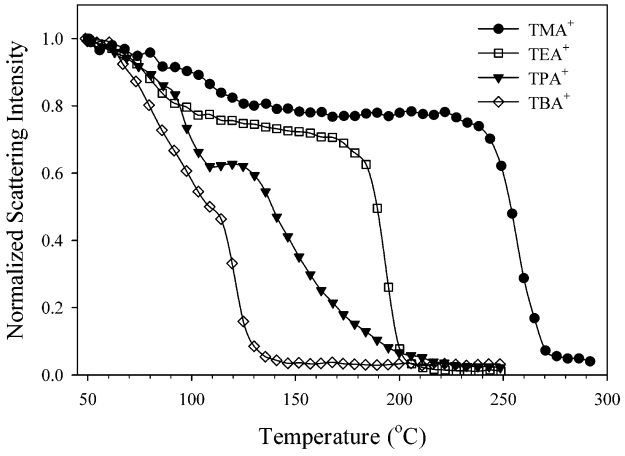

Figure 5. Normalized scattering intensity of the equatorial peak due to the ionic domains as a function of temperature for (●) TMA^+-, (□) TEA^+-, (▼) TPA^+-, and (◇) TBA^+-form Nafion.

increases and is quite narrow for TBA^+ Nafion. A comparison of the position of the tan δ peaks in the DMA with the second drop in intensity of the equatorial peak can be seen in Table 1. It is apparent that the second, larger drop in intensity correlates

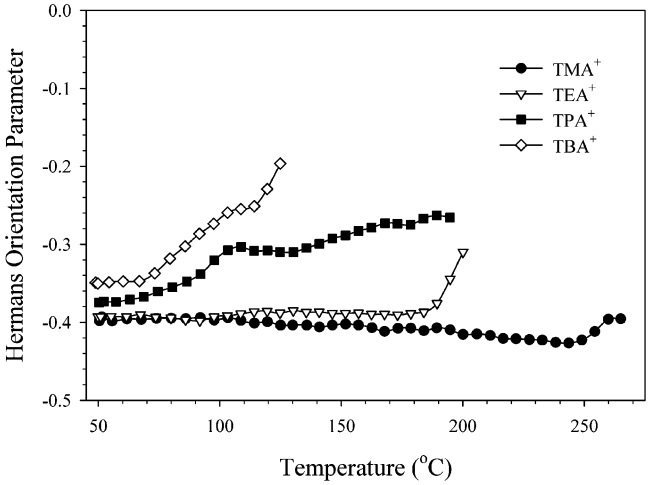

Figure 6. Hermans orientation function (*f*) vs temperature for (●) TMA^+-, (▽) TEA^+-, (■) TPA^+-, and (◇) TBA^+-form Nafion.

Table 1. Transition Temperatures (°C) Measured by DMA and SAXS for Oriented TMA^+, TEA^+, TPA^+, and TBA^+ Nafion

	DMA		
counterion form	α	β	SAXS
TMA^+	235	135	240−260
TEA^+	160	110	170−200
TPA^+	130	100	130−150
TBA^+	100	70	110−130

very well with the α relaxation in the DMA. These data are in excellent agreement with earlier studies showing a link between changes in the morphology and mechanical relaxations in unoriented Nafion films.[34]

A quantitative evaluation of the degree of orientation may be obtained using the Hermans orientation function (*f*) in order to assess the relaxation temperature of the anisotropic morphology. The Hermans orientation function (*f*) was calculated from the azimuthal plots seen in Figure 4 and is

$$f = \frac{3\langle\cos^2\chi\rangle - 1}{2} \tag{2}$$

where χ is the azimuthal angle and $\langle\cos^2\chi\rangle$ (the average squared of the cosine) is an expression of the orientation and can be calculated from the integral

$$\langle\cos^2\chi\rangle = \frac{\int_{\chi_1}^{\chi_2} I(\chi)\cos^2\chi\sin\chi\,d\chi}{\int_{\chi_1}^{\chi_2} I(\chi)\sin\chi\,d\chi} \tag{3}$$

where $I(\chi)$ is the scattering intensity as a function of χ and the limits of integration are between χ_1 and χ_2. The Hermans orientation function (*f*) assumes a value of 1 for a system with complete orientation of the scattering entities parallel to the director and $-1/2$ for the case where complete orientation of the scattering entities is perpendicular to the director. For samples with no orientation the value of *f* is zero. In the case of oriented Nafion it is necessary to clarify that the director is the momentum transfer vector (or scattering vector), *q*. If the orientation direction of the films is established as the primary axis, then the director, *q*, will be perpendicular to the orientation plane, resulting in values of *f* near $-1/2$.

The results of the Hermans orientation function calculations are shown in Figure 6, where *f* is plotted as a function of temperature for each of the neutralized forms of Nafion. At low temperatures, the initial value of *f* is seen to range between ca. −0.4 to −0.35, which indicates considerable orientation perpendicular to the orientation director as previously stated and in agreement with the literature. Also, the absolute value of the initial orientation parameter increases with decreasing counterion size (i.e., $|f| \rightarrow TMA^+ > TEA^+ > TPA^+ > TBA^+$), which indicates higher degrees of orientation for the smaller counterions. Again, this behavior can be accounted for by stress relaxation—facilitated by increased mobility due to counterion size—during the orientation and/or cooling process. For TMA^+ and TEA^+ Nafion, *f* remains relatively constant until ca. 250 and 190 °C, respectively. Above these temperatures *f* begins to approach zero (i.e., an isotropic, unoriented state) and becomes immeasurable due to the baseline noise. The transitions in *f* values for TPA^+ and TBA^+ Nafion are not as well defined but show a steady approach toward zero above 70 °C.

Together, the data in Figures 5 and 6 give a clear picture of the relaxation process for the anisotropic morphology of oriented Nafion films, and in correlation with our understanding of the dynamic mechanical relaxations in DMA,[34] it is evident that the morphological rearrangements observed at elevated temperatures are linked to the stability of the electrostatic network. As a direct comparison, the DMA and SAXS data for TMA^+

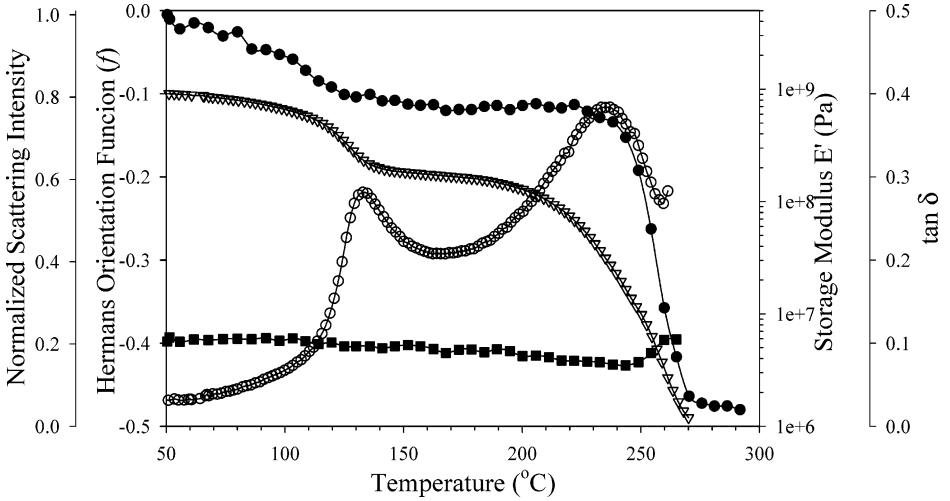

Figure 7. Correlations for TMA^+-form Nafion between the SAXS and DMA results showing the (●) normalized scattering intensity, (■) Hermans orientation function (*f*), (▽) storage modulus, and (○) tan δ.

Nafion are plotted together vs temperature in Figure 7. The initial decrease of the normalized scattering intensity of the equatorial peak for TMA^+ Nafion cannot be attributed to relaxation of the anisotropic morphology due to the fact that *f*, which is indicative of the degree of orientation, remains constant up to temperatures of ca. 250 °C. The initial drop in intensity correlates very well with the β relaxation observed in the storage modulus, as can be seen in Figure 7. Since the oriented morphology is not relaxing, the change in intensity can be explained as a result of a change in the contrast between the matrix and the ionic domains, which occurs due to relative density changes in the amorphous phase and the ionic domains. Therefore, these data demonstrate that Nafion is morphologically stable over temperature ranges in the vicinity of the β relaxation, which is attributed to the T_g of Nafion.

The dramatic decrease in the intensity between 240 and 260 °C (Figure 7) coincides with a change in *f* (i.e., *f* begins to increase toward zero), indicative of a relaxation of the anisotropic morphology. This relaxation also correlates well with the α relaxation observed in DMA. For Nafion containing large alkylammonium counterions (with significantly weakened interactions), the enhanced chain motions associated with the α relaxation may ultimately lead to a destabilization of the ionic domains (i.e., a transition from a static, physically cross-linked system to a dynamic network). At elevated temperatures, the elastic forces exerted upon the chains emanating from the ionic aggregates tend to increase to a point that exceeds the electrostatic attractive forces between ion pairs in the aggregate. As a result of this destabilizing condition, the static electrostatic network transitions to a dynamic network through the process known as ion-hopping (i.e., the thermally activated process of ion pairs "hopping" from one aggregate to another in order to relieve local stress).[35,36] This phenomenon creates a state of morphological instability in the oriented structure and thus facilitates the relaxation to an isotropic morphology at elevated temperatures.

Conclusions

The morphology of uniaxially oriented Nafion films was shown to be highly anisotropic characterized by strong equatorial scattering peaks located at approximately 90° and 270° (χ) with respect to the orientation direction. These peaks arise from correlations in the direction perpendicular to orientation and are attributed to orientation of the ionic domains parallel to the orientation direction. Analysis of the equatorial scattering intensity and the degree of orientation—through the Hermans orientation function (*f*)—in correlation with DMA results has led to a more precise description of the relaxation process. These data indicate that the α relaxation allows for the onset of long-range mobility of both the main and side chains facilitated by a profound weakening of the electrostatic interactions within the ionic aggregates. At temperatures in the vicinity of the α relaxation, a significant destabilization of the electrostatic network may be observed (i.e., through the activation of a *dynamic* network involving significant ion-hopping processes), thus facilitating relaxation to an isotropic morphology. In contrast, the β relaxation is associated with the onset of segmental motions (principally backbone motions) within the framework of a *static*, physically cross-linked network of chains. Since the oriented morphology persists at temperatures below the α relaxation, these data demonstrate that Nafion is morphologically stable over temperature ranges in the vicinity of the β relaxation, which is attributed to the to the T_g of Nafion. However, significant morphological instability, leading to possible structural rearrangement, is feasible in these ionomers if the application temperatures exceed the α relaxation.

While the use of this series of alkylammonium ions provides the necessary systematic variations in electrostatic interactions in order to elucidate the origins of morphological/mechanical relaxations in these ionomers, it is important to note that the principal application of Nafion (e.g., in PEM fuel cells) involves the H^+-form. Nevertheless, with this fundamental understanding of the link between morphological stability and chain dynamics, subsequent studies of the morphological behavior of Nafion in the H^+-form are likely to yield a deeper insight into the structural factors that may be controlled in order to yield more durable membranes with enhanced performance.

Acknowledgment. The authors acknowledge DuPont for providing the Nafion membranes. This work was supported by the MRSEC Program of the National Science Foundation under Award DMR 0213883. Additional support for this work was provided by the American Society for Engineering Education, National Defense Science and Engineering Graduate Fellowship. SAXS data were collected at the National Synchrotron Light Source, Brookhaven National Laboratory (supported in part by the U.S. Department of Energy, Division of Materials Sciences and Divison of Chemical Sciences, under Contract DE-AC02-98CCCCH10886).

References and Notes

(1) Grot, W. *Chem.-Ing.-Tech.* **1978**, *50*, 299.
(2) Yeo, R. S.; McBreen, J.; Kissel, G.; Kulesa, F.; Srinivasan, S. *J. Appl. Electrochem.* **1980**, *10*, 741.
(3) Mauritz, K. A.; Moore, R. B. *Chem. Rev.* **2004**, *104*, 4535−4583.
(4) Gierke, T. D.; Munn, G. E.; Wilson, F. C. *J. Polym. Sci., Polym. Phys. Ed.* **1981**, *19*, 1687−1704.
(5) Starkweather, H. W. *Macromolecules* **1982**, *15*, 320−323.
(6) Moore, R. B.; Martin, C. R. *Macromolecules* **1988**, *21*, 1334−1339.
(7) Fujimura, M.; Hashimoto, T.; Kawai, H. *Macromolecules* **1981**, *14*, 1309−1315.
(8) Fujimura, M.; Hashimoto, T.; Kawai, H. *Macromolecules* **1982**, *15*, 136−144.
(9) Gebel, G.; Lambard, J. *Macromolecules* **1997**, *30*, 7914−7920.
(10) Moore, R. B.; Martin, C. R. *Macromolecules* **1989**, *22*, 3594−3599.
(11) Roche, E. J.; Pineri, M.; Duplessix, R.; Levelut, A. M. *J. Polym. Sci., Polym. Phys. Ed.* **1981**, *19*, 1−11.
(12) Roche, E. J.; Pineri, M.; Duplessix, R. *J. Polym. Sci., Polym. Phys. Ed.* **1982**, *20*, 107−116.
(13) Elliot, J. A.; Hanna, S.; Elliot, A. M. S.; Cooley, G. E. *Macromolecules* **2000**, *33*, 4161−4171.
(14) Elliot, J. A.; James, P. J.; McMaster, T. J.; Newton, J. M.; Elliot, A. M. S.; Hanna, S.; Miles, M. J. Hydrolysis of the Nafion precursor studied by X-ray scattering and in-situ atomic force microscopy. http://www.e-polymers.org.
(15) Gebel, G.; Aldebert, P.; Pineri, M. *Macromolecules* **1987**, *20*, 1425−1428.
(16) Gebel, G.; Moore, R. B. *Macromolecules* **2000**, *33*, 4850−4855.
(17) Rollet, A.-L.; Diat, O.; Gebel, G. *J. Phys. Chem. B* **2002**, *106*, 3033−3036.
(18) Rubatat, L.; Rollet, A. L.; Gebel, G.; Diat, O. *Macromolecules* **2002**, *35*, 4050−4055.
(19) Almeida, S. H. D.; Kawano, Y. *J. Therm. Anal. Calorim.* **1999**, *58*, 569−577.
(20) Hodge, I. M.; Eisenberg, A. *Macromolecules* **1978**, *11*, 289−293.
(21) Kyu, T.; Hashiyama, M.; Eisenberg, A. *Can. J. Chem.* **1983**, *61*, 680−687.
(22) Moore, R. B.; Cable, K. M.; Croley, T. L. *J. Membr. Sci.* **1992**, *75*, 7−14.
(23) Yeo, S. C.; Eisenberg, A. *J. Appl. Polym. Sci.* **1977**, *21*, 875−898.

(24) Nakano, Y.; MacKnight, W. J. *Macromolecules* **1984**, *17*, 1585−1591.
(25) Moore, R. B.; Cable, K. M. *Polym. Prepr.* **1997**, *38*, 272−273.
(26) Barbi, V.; Funari, S. S.; Gehrke, R.; Scharnagl, N.; Stribeck, N. *Polymer* **2003**, *44*, 4853−4861.
(27) Cable, K. M.; Mauritz, K. A.; Moore, R. B. *Polym. Prepr.* **1994**, *35*, 421−422.
(28) Cable, K. M.; Mauritz, K. A.; Moore, R. B. *Chem. Mater.* **1995**, *7*, 1601−1603.
(29) Elliot, J. A.; Hanna, S.; Elliot, A. M. S.; Cooley, G. E. *Polymer* **2001**, *42*, 2251−2253.
(30) van der Heijden, P. C.; Rubatat, L.; Diat, O. *Macromolecules* **2004**, *37*, 5327−5336.
(31) Landis, F. A.; Moore, R. B.; Page, K. A.; Han, C. C. *Polym. Mater.: Sci. Eng.* **2002**, *87*, 121−122.
(32) Londono, J. D.; Davidson, R. V.; Mazur, S. *Polym. Mater.: Sci. Eng.* **2001**, *85*, 23−24.
(33) Cable, K. M.; Mauritz, K. A.; Moore, R. B. *Polym. Prepr.* **1994**, *35*, 854−855.
(34) Page, K. A.; Cable, K. M.; Moore, R. B. *Macromolecules* **2005**, *38*, 6472−6484.
(35) Kim, J. S.; Yoshikawa, K.; Eisenberg, A. *Macromolecules* **1994**, *27*, 6347−6357.
(36) Hird, B.; Eisenberg, A. *Macromolecules* **1992**, *25*, 6466−6474.

MA052359J